PHYSICAL REVIEW A VOLUME 27, NUMBER 1 JANUARY 1983

Extended zero-core-contribution model applied to multichannel photodetachment

W. B. Clodius, R. M. Stehman, and S. B. Woo
Physics Department, University of Delaware, Newark, Delaware 19711
(Received 17 February 1981)

The zero-core-contribution model is extended to calculate absolute photodetachment cross sections taking into account the fine-structure levels and higher electronic states of the anions and neutral atoms. Comparisons are made with experimental data involving 20 different anions with p outermost occupied orbitals. Very good agreement is obtained.

I. INTRODUCTION

The zero-core-contribution (ZCC) model[1] is extended to calculate absolute photodetachment cross sections taking into account the fine-structure levels and higher electronic states of the anions and neutral atoms. Comparisons are made with experimental data involving 20 different anions.

The zero-core-contribution model is an attempt to create a simple but reasonable model for calculating photodetachment characteristics of anions. It is a one-electron model. It depicts a negative ion of many indistinguishable electrons in terms of an "equivalent" system of a neutral atom and an extra electron. The wave function of this "extra electron" outside a radius r_0 is obtained by solving the constant potential Hamiltonian with the correct angular momentum value. Inside the radius r_0 the wave function is identically zero. We choose $r_0=1.3\langle R^2\rangle^{1/2}$, where $\langle R^2\rangle^{1/2}$ is the root-mean-square radius of the outermost occupied orbital in the neutral atom taken from Lu *et al.*[2] Three factors combine to make this simple model successful for calculating absolute photodetachment cross sections. First, the electron affinity is small compared with the energy required to form a positive ion. This implies that the probability of the extra electron being within r_0 cannot be very large. Secondly, the dipole length operator emphasizes the contribution to photodetachment from larger radial distances. These two factors permit the use of the spherical-well wave function which is asymptotically correct but which has a zero core. Thirdly, the "shift in phase" appropriate for photodetachment is not the total phase shift at $r=\infty$, which results largely from long-range interactions such as polarization. Only the smaller shift in phase accumulated at intermediate radial distance, where the contribution to photodetachment is significant, is required. We do not specifically treat this shift in phase.

The zero-core-contribution model is versatile and easy to apply. It requires only three input values—r_0, E, and l. E is the threshold energy for each photodetachment channel. l is the orbital quantum number of the extra electron. Information about these parameters is readily available,[1] allowing the model to be applied to a wide variety of anions. It calculates the angular distribution of photodetached electrons. It calculates the absolute photodetachment cross section to better than a factor of 2 accuracy.

II. EXTENDED ZERO-CORE-CONTRIBUTION MODEL

The differential photodetachment cross section from the initial state of an anion of given $(\mathcal{L},\mathcal{S},\mathcal{J},\mathcal{M}_{\mathcal{J}})$ to a final state of an atom of given (L',S',J',M_J') plus a free electron of given $(\vec{k},m_s')$ is shown in the Appendix, subsection 1, as

$$\frac{d\sigma_1}{d\Omega}(\vec{k},m_s',L',S',J',M_J',\mathcal{L},\mathcal{S},\mathcal{J},\mathcal{M}_{\mathcal{J}})$$

$$=(2\pi)^2\frac{e^2}{\hbar c}\frac{m_e k\omega}{\hbar}\left|\sum_{M_S,M_L}C_{LS}(\mathcal{J},\mathcal{M}_{\mathcal{J}};\mathcal{M}_{\mathcal{S}},\mathcal{M}_{\mathcal{L}})\sum_{M_L',M_S'}C_{L'S'}(J',M_J';M_L',M_S')\langle l^n(S',L')\}\mathcal{S},\mathcal{L},\rangle\right.$$

$$\left.\times C_{L'l}(\mathcal{L},\mathcal{M}_{\mathcal{L}};M_L',\mathcal{M}_{\mathcal{L}}-M_L')C_{S'1/2}(\mathcal{S},\mathcal{M}_{\mathcal{S}};M_S',m_s')\langle\psi_k(\vec{r})\,|\,\hat{e}\cdot\vec{r}\,|\,\psi_l(\vec{r},m_l)\rangle\right|^2, \tag{1}$$

where $(\mathscr{L},\mathscr{S},\mathscr{J},\mathscr{M}_{\mathscr{J}})$ and (L',S',J',M_J') are, respectively, the orbital angular momentum, spin, total angular momentum, and z component of the total angular momentum of the anion and of the atom. m_e, ω, and k are, respectively, electron mass, photon angular frequency, and momentum wave number of the detached electron. $e^2/\hbar c$ and C are, respectively, the fine-structure constant and Clebsch-Gordan coefficients. $\hat{e}$ is the polarization unit vector. $\langle l^n(S',L')l\}\mathscr{S},\mathscr{L}\rangle$ is the fractional parentage coefficient,[3] where l is the electron orbital angular momentum of the outer shell of the anion. n is the number of electrons in the outer shell of the neutral. $\psi_l(\vec{r})$ and $\psi_k(\vec{r})$ are, respectively, the one-electron detachment orbital wave function described in the Appendix and Ref. 1 and the one-electron wave function describing the detached free electron. ψ_l and ψ_k do not include the spin function.

The total cross section is the integral over $d\Omega$ of the differential cross section. For a particular coordinate system, the following substitutions can be used:

$$\psi_k(\vec{r})=(2\pi)^{-3/2}e^{i\vec{k}\cdot\vec{r}}=(2\pi)^{-3/2}e^{-ikz}$$

$$=(2\pi)^{-3/2}\sum_{l=0}^{\infty}(2l+1)^{1/2}i^l j_l(kr)Y_l^0(\theta,\phi)\ , \tag{2}$$

$$\hat{e}\cdot\vec{r}=r\cos\theta'=(4/3)\pi r\sum_{m=-1}^{1}Y_1^m(\chi,\xi)Y_1^m(\theta,\phi)\ , \tag{3}$$

and

$$\psi_l(\vec{r},m_l)=Y_l^{m_l}(\theta,\phi)R_l(r)\ , \tag{4}$$

where χ and ξ are the polar angles describing the orientation of $\hat{e}$ with respect to $\vec{k}$. $R_l(r)$ is zero within the core region. For $r>r_0$, it satisfies

$$\frac{1}{r^2}\frac{d}{dr}r^2\frac{dR_l}{dr}-\frac{l(l+1)R_l}{r^2}=\gamma^2R_l\ , \tag{5}$$

where $\gamma=\sqrt{2mE}/\hbar$ and E is the energy required to go from an initial electronic state of an anion of given $(\mathscr{L},\mathscr{S},\mathscr{J})$ to a final electronic state of its neutral atom with specified (L',S',J'). E is no longer necessarily the electron affinity. Subsequently, one obtains

$$\begin{aligned}\sigma_1(k,m_s',L',S',J',M_J',\mathscr{L},\mathscr{S},\mathscr{J},\mathscr{M}_{\mathscr{J}})=&\frac{8\pi^2}{3(2l+1)}\frac{e^2}{\hbar c}\frac{m_l k\omega}{\hbar}\,|\langle l^n(S',L')l\}\mathscr{S},\mathscr{L}\rangle|^2\\ &\times\sum_{m=-1}^{1}\Big|[(2l-1)\langle j_{l-1}(kr)\,|\,r\,|\,R_l(r)\rangle C_{l-1,1}(l,m;0,m)\\ &\times C_{l-1,1}(l,0;0,0)-(2l+3)\langle j_{l+1}(kr)\,|\,r\,|\,R_l(r)\rangle\\ &\times C_{l+1,1}(l,m;0,m)C_{l+1,1}(l,0;0,0)]\\ &\times\sum_{M_LM_S}C_{\mathscr{L}\mathscr{S}}(\mathscr{J},\mathscr{M}_{\mathscr{J}};\mathscr{M}_{\mathscr{L}},\mathscr{M}_{\mathscr{S}})\\ &\times\sum_{M_L',M_S'}C_{L'S'}(J',M_J';M_L',M_S')C_{L'l}(\mathscr{L},\mathscr{M}_{\mathscr{L}};M_L',-m)\\ &\times C_{S',1/2}(\mathscr{S},\mathscr{M}_{\mathscr{S}};M_S',m_s')\Big|^2\ .\end{aligned} \tag{6}$$

For anions with a p outermost occupied orbital, l equals unity. Then the two radial matrix elements $\langle j_{l-1}\,|\,r\,|\,R_l\rangle$ and $\langle j_{l+1}\,|\,r\,|\,R_l\rangle$ will be equal to the expressions for R_{sp} and R_{dp} shown in Eqs. (17a) and (17b) of Ref. 1.

Normally the $\mathscr{M}_{\mathscr{J}}$ of the anion, the M_J' of the neutral atom, and the spin alignment of the photodetached electrons m_s' are not specified in the dis-

TABLE I. Parameters employed for the calculation of cross sections.

Ion	r_0 (Å)[a]	EA (eV)[b]	T (K)[c]	Ground term	Excitation energy (eV) to reach the specified term	
					$^3P_1$	$^3P_2$
B	1.78	0.28		$^3P_0$	0.001	0.003
Ga	2.56	0.3	1100	$^3P_0$	0.027	0.072
In	2.70	0.3	1100	$^3P_0$	0.085	0.192
Tl	2.42	0.3		$^3P_0$		
					$^2D_{3/2}$	$^2D_{5/2}$
C	2.56	1.268		$^4S_{3/2}$		
Si	2.06	1.385	10000	$^4S_{3/2}$	0.862[d]	0.863[d]
Ge	2.11	1.2	4000	$^4S_{3/2}$	0.78[e]	0.80[e]
Sn	2.29	1.15[f]	4000	$^4S_{3/2}$	0.65[e]	0.75[e]
					$^3P_1$	$^3P_0$
P	1.73	0.7468[g]	3000	$^3P_2$	0.0225[g]	0.0326[g]
As	1.87	0.81[h]	3000	$^3P_2$	0.136[h]	0.186[h]
Sb	2.14	1.07[h]	3000	$^3P_2$	0.335[h]	0.372[h]
Bi	2.36	0.9[h]	3000	$^3P_2$	0.6[h]	0.65[h]
					$^2P_{1/2}$	
O	0.96	1.462		$^2P_{3/2}$	0.022	
S	1.50	2.0772	1400	$^2P_{3/2}$	0.0697	
Se	1.67	2.0206	1700	$^2P_{3/2}$	0.2826	
Te	1.94	1.9708	3000	$^2P_{3/2}$	0.6209	
F	0.89	3.399		^1S		
Cl	1.34	3.615		^1S		
Br	1.52	3.364		^1S		
I	1.79	3.061		^1S		

[a] $r_0 = 1.3\langle R^2\rangle^{1/2}$, with $\langle R^2\rangle^{1/2}$ from Ref. 2.
[b] Unless otherwise stated, the electron affinities and ion excitation energies are from the review by Hotop and Lineberger, Ref. 4.
[c] The temperatures for S^- and Se^- are estimated by the experimental groups of their ion source conditions. The temperatures for B^-, C^-, O^-, F^-, Cl^-, Br^-, and I^- are not specified because the fine-structure splittings in their ground states are small as compared with room-temperature thermal energy, or because there is no splitting. The temperatures for other ions are chosen to give reasonable agreement between the ZCC theory and the experimental data.
[d] Mean ^2D energy from Ref. 5, splitting of ^2D levels from Ref. 4.
[e] Mean ^2D energy from Ref. 6, splitting of ^2D levels from Ref. 4.
[f] Reference 6.
[g] Reference 7.
[h] Reference 8.

cussions of a detachment channel. A specific photodetachment channel connects a term $(\mathcal{L},\mathcal{S},\mathcal{J})$ of the anion and a term (L',S',J') of the resulting neutral. Therefore, the cross section for such a single channel is obtained by averaging over the degenerate states $\mathcal{M}_\mathcal{J}$ and summing over the degenerate states of the atom M_J' and spin states of the outgoing electron m_s':

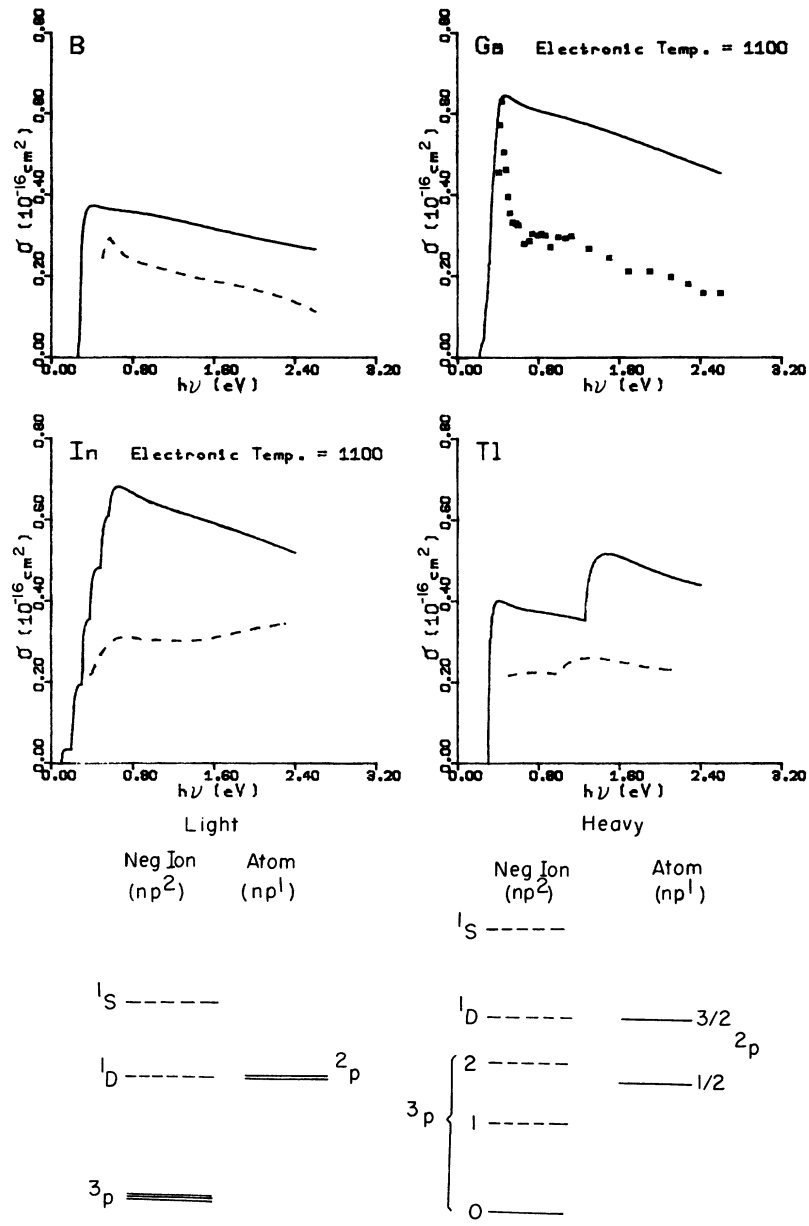

FIG. 1. Photodetachment cross sections and typical energy-level diagrams for ions and atoms of the boron column in the periodic table. The solid lines show calculated cross sections. Experimental data, having an energy resolution of 0.15 eV, are represented by dots or dashed lines. The dashed lines in the level diagram indicate that the level could be higher than the atomic ground level and should autodetach.

$$\sigma_2(k,L',S',J',\mathscr{L},\mathscr{S},\mathscr{J})=\frac{1}{(2\mathscr{J}+1)}\sum_{M_{\mathscr{J}}}\sum_{M_J'}\sum_{m_s'}\sigma_1 . \tag{7}$$

If the ions initially have a population distributed among several terms, then

$$\sigma(L',S',J')=\sum_{\mathscr{L},\mathscr{S},\mathscr{J}}\rho(\mathscr{L},\mathscr{S},\mathscr{J})\sigma_2 , \tag{8}$$

where ρ is the fraction of ion population in the term $(\mathscr{L},\mathscr{S},\mathscr{J})$. In the work seen in Sec. III, the fraction of ions populating a given term $(\mathscr{L},\mathscr{S},\mathscr{J},)$ is taken to be proportional to the statistical weight $2\mathscr{J}+1$ and the Boltzmann factor.

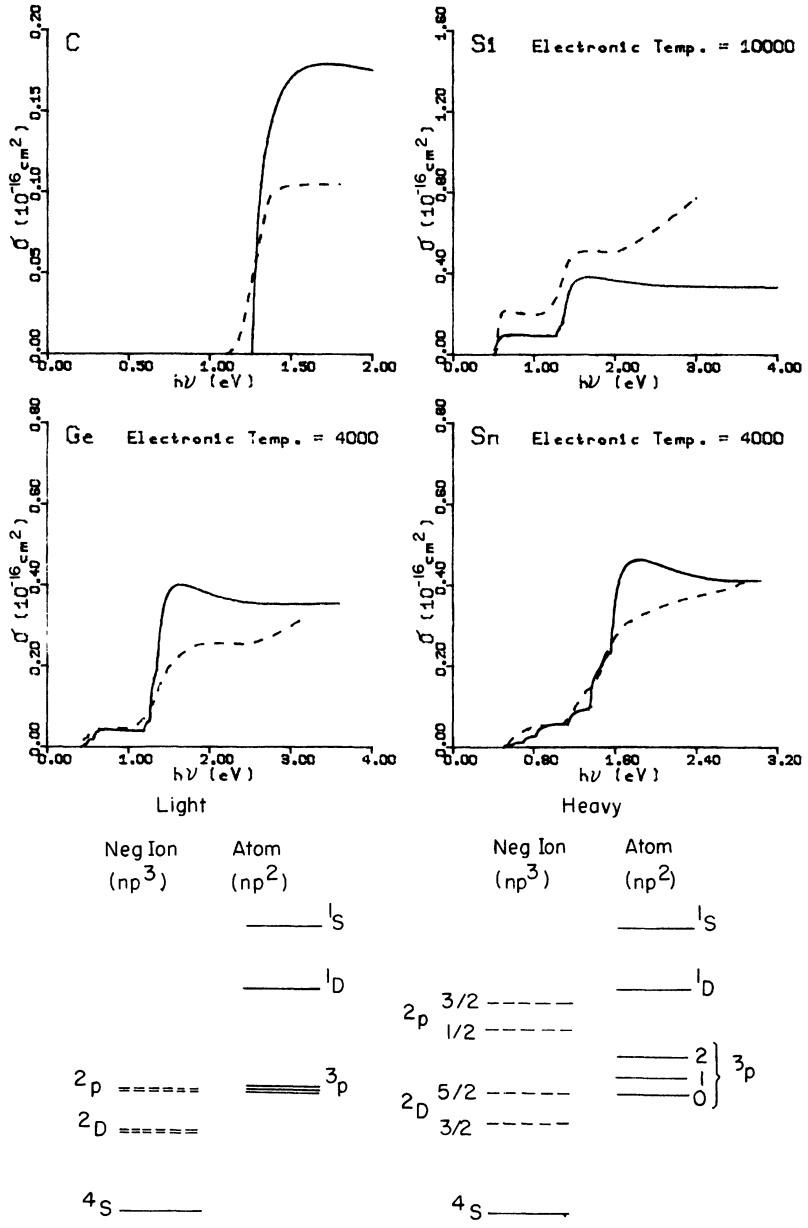

FIG. 2. Photodetachment cross sections and typical energy-level diagrams for ions and atoms of the carbon column. The energy resolution of the experimental data is 0.15 eV. Notations are the same as in Fig. 1.

III. COMPARISON WITH EXPERIMENTS

Comparison is made for 20 different ions having p outermost occupied orbitals. We compare our theory with only one set of data for each ion to avoid cluttering the figures. When data from several experimental groups are available for the same ion, the choice is usually in favor of data from the experimental group having data for the largest number of ions regardless of the quality of agreement with theory. Five figures are shown. Each compares the results for four ions from one column of the periodic table. Energy-level diagrams are shown in the bottom of each figure. The one on the left is representative of energy levels of light elements of that column. The one on the right is typical for heavy elements.

The electron affinities and excited-term energy

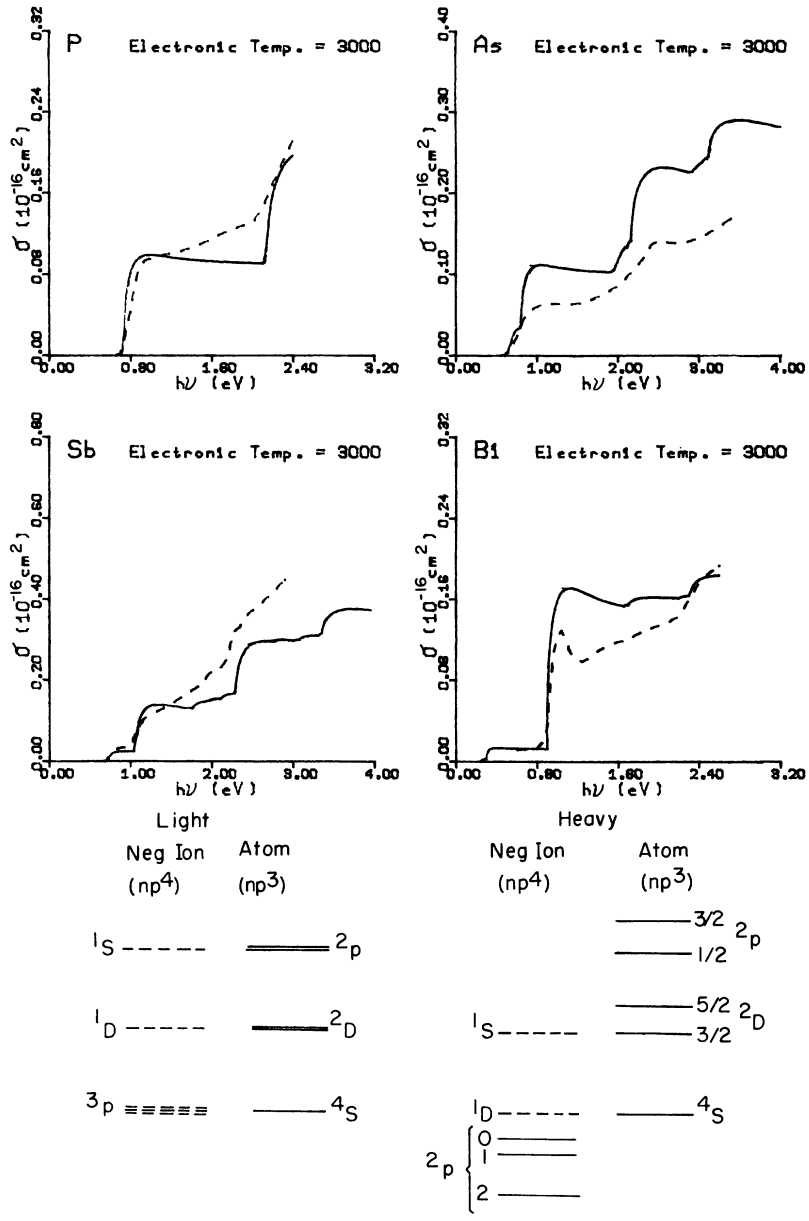

FIG. 3. Photodetachment cross sections and typical energy-level diagrams for ions and atoms of the nitrogen column. The energy resolution of the experimental data is 0.15 eV. Notations are the same as in Fig. 1.

levels of the anions used to determine the thresholds for all the channels of the 20 ions considered in this work are given in Table I. Excited-term energy levels of neutral atoms are available in standard references and are therefore not listed. Entries which are left blank indicate that the corresponding quantity is insignificant (e.g., terms of the ions which are not bound or undergo autodetachment). For ions which have more than one bound term, Table I gives the temperature we have employed to determine the initial distribution of the ions, $\rho(\mathscr{L},\mathscr{S},\mathscr{J})$. These temperatures are, when available, estimates provided by the experimental groups with whose data we make comparison. Otherwise, the temperature has been chosen to yield best agreement with the experimental data.

Figure 1 compares the photodetachment cross section of ions of the boron group. The experimental data, shown as dots or in dashed lines, are taken from those of Feldmann *et al.*[6] The solid lines

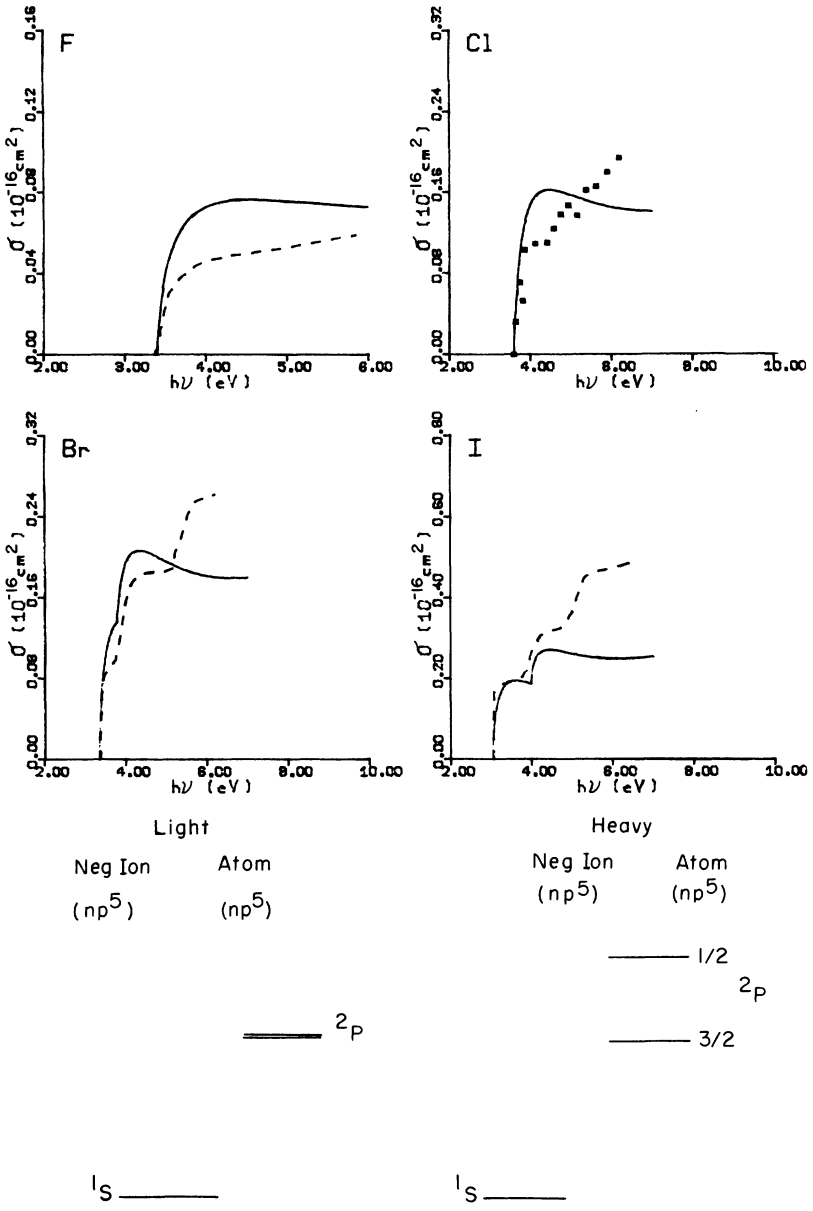

FIG. 4. Photodetachment cross sections and typical energy-level diagrams for ions and atoms of the fluorine column. The energy resolution of the experimental data is about 0.03 eV. Notations are the same as in Fig. 1. The experimental data is independent of temperature since there is only one electronic state for the anion.

show the calculated cross section. Feldmann's data have an energy resolution[9] of about 0.15 eV. This accounts for the presence of onsets seen in the calculated curve but not in the data of In. It also causes the onset of the second channel in Tl to shift to a lower energy. Otherwise, the shapes of cross sections agree well. The agreement of the absolute magnitudes is within the estimated error of the experiment and the theory. The estimated uncertainty of the experimental data is $\pm 50\%$.

Figure 2 compares cross sections for ions of the carbon group. The data shown are by Feldmann[5,10] and Feldmann *et al.*[6] and have an estimated error of $\pm 50\%$. The energy resolution is about 0.15 eV, which again causes the apparent onset of higher photodetachment channels to shift towards lower energies. The data for tin (Sn) was given in arbitrary units.[6] We normalize this set of experimental data to agree with the calculation near the middle of the energy range of the data. The agreement be-

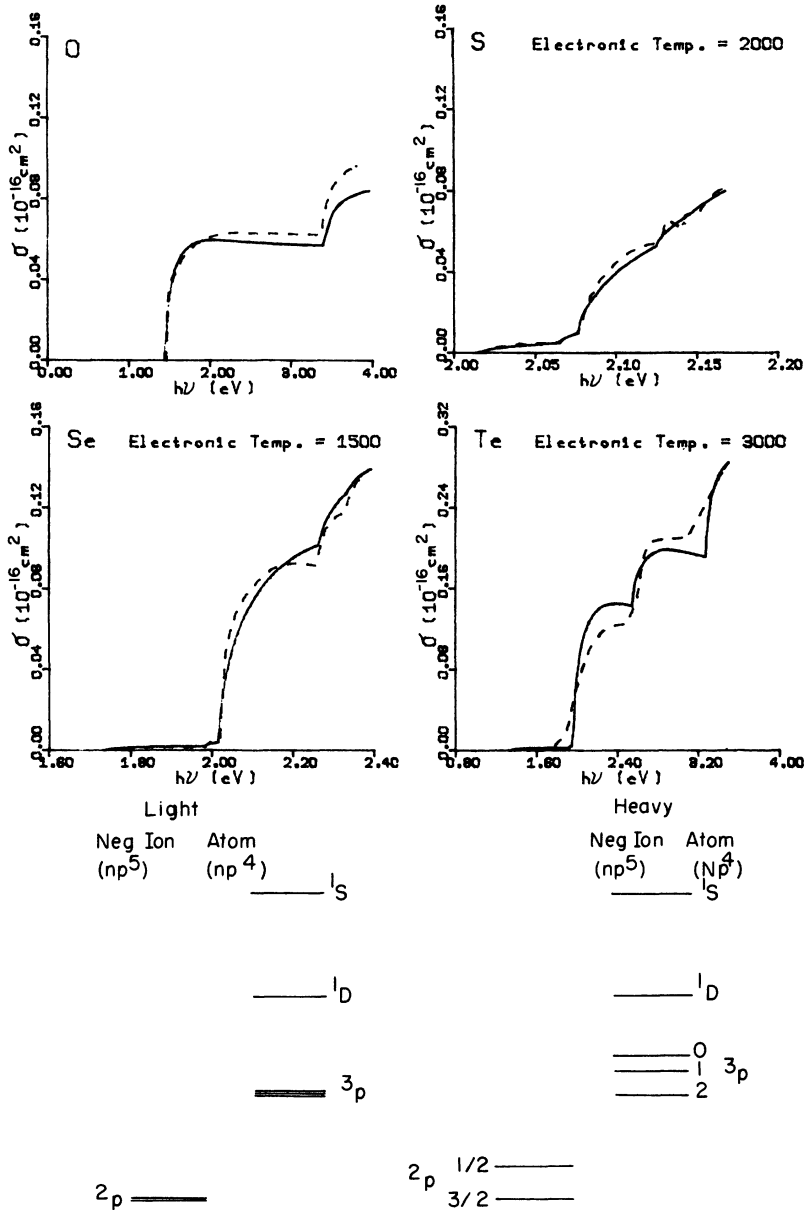

FIG. 5. Photodetachment cross sections and typical energy-level diagrams for ions and atoms of the oxygen column. The data on S^- and Se^- are obtained with dye lasers as light sources. The energy resolution of the Te data is about 0.15 eV. Notations are the same as in Fig. 1.

tween theory and experiment for carbon is very good for the data of Seman and Branscomb,[11] but not as good for the data shown. The agreement for the other three ions is within ±50%. It should be noted that the "electronic temperature" we have inferred for silicon is especially high. This may be because the high current arc used to produce this ion[5] may favor formation of Si^- in an excited state. Thus, the initial populations of excited states may not be described by a Boltzmann distribution.

Figure 3 compares cross sections for ions in the phosphorous column. The data are again from Feldmann *et al.*[8] having ±50% uncertainty. The low resolution again caused the shift in the onsets to lower energies. The agreement between theory and experiment is very good.

Figure 4 compares cross sections for ions of the fluorine group. The data shown for fluorine, chlorine, and bromine are those of Mandl.[12,13] The data shown for iodine are those of Mandl and Hy-

man.[14] Their energy resolution is about 0.03 eV. The uncertainty is ± 25%. The magnitudes predicted by the theory agree very well with those of the data shown. The shapes of cross sections agree moderately well. One might also note that the measurements of the same cross sections by others[15–19] are appreciably different from some of Mandl's.

Figure 5 presents cross sections for ions in the oxygen column. Experimental data for oxygen, sulfur, selenium, and tellurium are obtained, respectively, from Branscomb *et al.*,[20] Lineberger *et al.*,[21] Hotop *et al.*,[22] and Feldmann *et al.*[8] The photodetachment cross section of oxygen is probably one of the most carefully determined measurements. It is gratifying to find that theory and experiment are in excellent agreement in both magnitude and shape for oxygen. The relative measurements for the other three ions also show excellent agreement with the theory when each is normalized at the midpoint of its energy range. Data from the Feldmann group[8] for Te again show the anticipated low-energy shift of onsets. The dye laser data on sulfur[21] and selenium[22] are not subject to such a shift and therefore show good agreement with the theory. In the case of sulfur, the ZCC theory shows excellent agreement with data from Lineberger *et al.*[21] It is also in good agreement with the theory of Rau and Fano.[23] Excellent agreement is also found in the case of selenium between the ZCC calculation and Hotop's measurement and calculations.[22] Hotop *et al.* made one absolute photodetachment determination for Se. They found the cross section for the channel $Se^-(^2P_{3/2}) \rightarrow Se(^3P_2)$ at 18 000 cm^{-1} to be $(7.5\pm2)\times10^{-18}$ cm^2. The ZCC value is 9.07×10^{-18} cm^2. Transition strengths for various fine-structure onsets in Se^- were measured by Hotop *et al.*[22] Of the theoretical models with which they compared, their values agree best with those of Rau and Fano. The ZCC transition strengths are identical to those of Rau and Fano.

IV. CONCLUSION

Good agreement is shown between the predictions of the zero-core-contribution model and the experimental data involving 20 different anions of p outermost occupied orbital. Fine-structure levels and higher electronic states of the anions and neutral atoms are taken into account.

Besides the explicit assumption of a zero core, the model makes use of several additional simplifying assumptions. It assumes that the ions can be described by an independent electron model. It assumes that the ion is adequately described by a neutral atomic core which is L-S coupled to the additional electron. It assumes that the free electron, after photodetachment, is adequately described by a plane wave and that the effect of ignoring the shift in phase is small. It assumes that the bound electron's wave function is adequately described by an asymptotic wave function with a zero-core cutoff. Lastly, it assumes a photodetachment process which detaches an electron from the outermost orbital and which otherwise does not change the electronic configurations of the anion.

The agreement between theory and experimental data shows that the ZCC model is a simple but generally realistic model of the photodetachment process. To the best of our knowledge it is the first model that has the ability to predict absolute photodetachment cross sections for all p-orbital atomic ions. Further, the results of this theory compare quite well with the other more complicated theories which are practical for only one or, at most, a few particular atomic anions.

The success of the ZCC model depends a great deal on the diffuse nature of the negative-ion orbital coupled with the use of the dipole length operator. One might therefore suspect that a simple model potential approach, such as a spherical square-well approach, may be equally successful. However, after investigation we found that the calculated results would not agree with experimental cross sections unless the parameters of the model potential were chosen for each anion in an *ad hoc* fashion. This is because a simple model potential approach often produces a bound-state wave function that is too large inside the well which, in turn, requires the *ad hoc* adjustment of parameters to fit the experimental data. In other words, the assumption of a zero core, albeit an oversimplification, is an essential element in the success of this type of calculation which focuses on the asymptotic behavior of the bound-state wave function.

The ZCC model has recently been successfully extended to study the photodetachment of homonuclear diatomic anions, taking into explicit account the vibrational motions of both the anions and molecules.[24] It is currently being applied to heteronuclear diatomic and triatomic anions. The preliminary results are in very good agreement with existing experimental data. Needless to say, the ZCC model is not a complete description of the physics of negative ions. A discussion of its limitations is seen in Ref. 1.

ACKNOWLEDGMENTS

We wish to thank Dr. E. M. Helmy for her valuable assistance. This work was supported in part by the National Science Foundation Grant No. ATM-77-18324 and Army Research Office Grant No. DAAG29-81-G-0001.

APPENDIX: RELATIONSHIP BETWEEN $(n+1)$-ELECTRON AND ONE-ELECTRON MATRIX ELEMENTS

This appendix shows that the photodetachment cross section can, to a good approximation, be computed using one-electron wave functions in accordance with Eq. (1). Three things must be investigated: (a) the structure of the $n+1$ electron bound-state wave function of the ion, (b) the structure of the $n+1$ electron continuum final-state wave function, and (c) the structure of the matrix element connecting these multielectron initial- and final-state wave functions.

To simplify our analysis, we assume that only the outer shell of the ion and atom need be considered, and all other shells are completely filled. We introduce the following notation. Since only the outer shell is considered, n will denote the number of outer-shell electrons of the atom. $\Psi(L,S,M_L,M_S;1,\ldots,n)$ denotes the wave function of the outer shell of the atom having total orbital angular momentum L with z component M_L, and total spin S with z component M_S. The indices $1,\ldots,n$ represent the spatial and spin coordinates of the n electrons of the outer shell of the atom. $\Psi_i(\mathscr{L},\mathscr{S},\mathscr{J},\mathscr{M}_\mathscr{J};1,\ldots,n+1)$ denotes the wave function of the outer shell of the ion having total angular momentum $\mathscr{J}$ with z component $\mathscr{M}_\mathscr{J}$, total spin $\mathscr{S}$, and total orbital angular momentum $\mathscr{L}$. $\phi(m_l,m_s;r,\sigma)$ is a one-electron atomic orbital belonging to the outer shell of the atom. The one-electron orbital momentum characterizing this shell is l, and the z component of the orbital angular momentum and spin are m_l and m_s, respectively. r denotes the spatial coordinate of the electron and σ denotes the two-valued spin coordinate. $\psi_l(m_l;r)$ is the detachment orbital and $\psi_k(r)$ is the one-electron wave function describing the detached electron. ψ_l and ψ_k do not include the spin function.

The atomic orbitals have the form

$$\phi_l(m_l,m_s;\vec{r},\sigma)=u_l(r)Y_{lm_l}(\theta,\phi)\chi_{m_s}(\sigma)\ , \qquad \text{(A1)}$$

where u_l is the radial function common to all the outer-shell atomic orbitals, $Y_{lm_l}(\theta,\phi)$ is the spherical harmonic of degree l and order m_l, and $\chi_{m_s}(\sigma)$ is a two-component spinor. The detachment orbital has a different radial function than the atomic orbitals:

$$\psi_l(m_l,\vec{r})=R_l(r)Y_{lm_l}(\theta,\phi)\ , \qquad \text{(A2)}$$

where R_l is the detachment orbital's radial function.

The atomic wave function $\Phi(L,S,M_L,M_S;1,\ldots,n)$ is constructed from the set of one-electron orbitals $\phi_l(m_l,m_s;r,\sigma)$. This is done by taking linear combinations of $n\times n$ Slater determinants,[25] the linear combination being chosen to give the desired total L, S, M_L, and M_S. The resulting wave function can be factored:

$$\Phi(L,S,M_L,M_S;1,\ldots,n)=u_l(r_1)\cdots u_l(r_n)W(L,S,M_L,M_S;\theta_1\cdots\theta_n,\phi_1\cdots\phi_n,\sigma_1\cdots\sigma_n)\ , \qquad \text{(A3)}$$

where the function W contains all the combinations of spherical harmonics and spin functions that appear in the determinants.

1. Ion wave function

The wave function of the ion Ψ_i is constructed by combining the atomic wave function Φ of Eq. (A1) with the detachment orbital ψ_l. $\Psi_i(\mathscr{L},\mathscr{S},\mathscr{J},\mathscr{M}_\mathscr{J};1,\ldots,n+1)$ must satisfy the following three conditions.

(i) It must be an eigenstate of the ion's total orbital angular momentum and the ion's total spin.

(ii) It must be antisymmetric with respect to exchange of the coordinates of any two electrons.

(iii) It must conform to a configuration of $n+1$ equivalent electrons.[26]

Such a wave function can be found, employing the concept of fractional parentage[27]

$$\psi_i(\mathscr{L},\mathscr{S},\mathscr{J},\mathscr{M}_\mathscr{J};1,\ldots,n+1)$$

$$=N\sum_{j=1}^{n+1}u_l(r_1)\cdots R_l(r_j)\cdots u_l(r_{n+1})\sum_{\mathscr{M}_\mathscr{S}+\mathscr{M}_\mathscr{L}=\mathscr{M}_\mathscr{J}}C_{LS}(\mathscr{J},\mathscr{M}_\mathscr{J},\mathscr{M}_\mathscr{L},\mathscr{M}_\mathscr{S})\sum_{L,S}\langle l^n(S,L)l\}\mathscr{S},\mathscr{L}\rangle$$

$$\times\sum_{m_l+M_L=\mathscr{M}_\mathscr{L}}\sum_{m_s+M_S=\mathscr{M}_\mathscr{S}}C_{Ll}(\mathscr{L},\mathscr{M}_\mathscr{L};M_Lm_l)C_{Ss}(\mathscr{S},\mathscr{M}_\mathscr{S};M_Sm_s)$$

$$\times W(L,S,M_L,M_S;1,\ldots,n)Y_{lm}(\theta_{n+1},\phi_{n+1})\chi_{m_s}(\sigma_{n+1})\,, \tag{A4}$$

where $\langle(S,L)l\}\mathscr{S},\mathscr{L}\rangle$ is the fractional parentage coefficients. Standard procedure to evaluate the normalization coefficient N yields

$$N^2=\left\{(n+1)\left[1+n\left[\int u_l(r)R_l(r)r^2dr\right]^2\right]\right\}^{-1}\cong(n+1)^{-1}\,, \tag{A5}$$

since it is a basic assumption of the ZCC model that the overlap integral of u_l and R_l is negligibly small.

2. Final-state wave function

The final-state wave function describes an atom having total angular momentum J' with z component M_J', total spin S', and total orbital angular momentum L' together with a detached electron escaping with momentum $\vec{k}$ and z component of spin m_s'. An antisymmetric wave function describing this state is

$$\Psi_f(L',S',J',M_J',\vec{k},m_S')$$

$$=\frac{1}{\sqrt{n+1}}\left[\sum_{M_L'+M_S'=M_J'}C_{L'S'}(J',M_J',M_L',M_S')\left[\psi_k(\vec{r}_{n+1})\chi_{m_S'}(\sigma_{n+1})\Phi(L',S',M_L',M_S';1,\ldots,n)\right.\right.$$

$$\left.\left.-\sum_{j=1}^{n}\Phi(L',S',M_L',M_S';j\leftrightarrow n+1)\psi_k(\vec{r}_j)\chi_{m_s'}(\sigma_j)\right]\right]. \tag{A6}$$

The symbol

$$\Phi(L',S',M_L',M_S';j\leftrightarrow n+1)$$

denotes the function

$$\Phi(L',S',M_L',M_S';1,\ldots,j-1,n+1,j+1,\ldots,n)\,,$$

the coordinates of the jth electron having been replaced by those of the $(n+1)$st electron. The terms containing

$$\Phi(L',S',M_L',M_S';j\leftrightarrow n+1)$$

make Ψ_f antisymmetric with respect to exchange of any pair of electrons, since Φ is antisymmetric.

3. Reduction of the matrix element

The differential photodetachment cross section is

$$\frac{d\sigma_1}{d\Omega}=(2\pi)^2\frac{e^2}{\hbar c}\frac{m_ek\omega}{\hbar}|M_{fi}|^2\,, \tag{A7}$$

where

$$M_{fi}=\left\langle \Psi_f(L',S',J',M_J',k,m_S';1,\ldots,n+1)\right|\times\sum_{j=1}^{n+1}\hat{e}\cdot\vec{r}_j\left|\Psi_i(\mathscr{L},\mathscr{S},\mathscr{J},\mathscr{M}_{\mathscr{J}};1,\ldots,n+1)\right\rangle . \tag{A8}$$

Algebraic manipulation and application of Eqs. (A9)–(A12), shown below,

$$\langle\phi_l(\vec{r}_j)\,|\,\vec{r}_j\,|\,\phi_l(\vec{r}_j)\rangle=\langle\phi_l(\vec{r}_j)\,|\,\vec{r}_j\,|\,\psi_l(\vec{r}_j)\rangle\equiv 0\,, \tag{A9}$$

$$\langle u_l(r)\,|\,R_l(r)\rangle\cong 0\,, \tag{A10}$$

$$\langle\psi_k(\vec{r})\chi_{m_S'}(\sigma)\,|\,\hat{e}\cdot\vec{r}\,|\,\psi_l(\vec{r},m_l)\chi_{m_S}(\sigma)\rangle=\langle\psi_k\,|\,\hat{e}\cdot\vec{r}\,|\,\psi_{lm_l}\rangle\delta_{m_Sm_S'}\,, \tag{A11}$$

and

$$\langle\Phi(L',S',M_L',M_S')\,|\,\Phi(L,S,M_L,M_S)\rangle=\delta_{L'L}\delta_{S'S}\delta_{M_L'M_L}\delta_{M_S'M_S} \tag{A12}$$

reduce Eq. (A7) to the explicit expression shown in Eq. (1).

Implicit in Eq. (A12) is the assumption that the photodetachment process does not change the electronic configurations of the anion beyond the removal of one electron from the outermost occupied orbital. A result equivalent to Eq. (1) can also be obtained from the approach of Rau and Fano[23] and Engelking *et al.*[28] who applied the 9-J symbol. However, the discussion shown in this appendix helps to clarify the assumptions of the one-electron approach as applied to our ZCC model.

[1]R. M. Stehman and S. B. Woo, Phys. Rev. A 20, 281 (1979).
[2]C. C. Lu, T. A. Carlson, F. B. Malik, T. C. Tucker, and C. W. Nestor, Jr., At. Data 3, 1 (1971).
[3]G. Racah, Phys. Rev. 63, 171 (1943).
[4]H. Hotop and W. C. Lineberger, J. Phys. Chem. Ref. Data 4, 539 (1975).
[5]D. Feldmann, Z. Naturforsch. 26a, 1100 (1971).
[6]D. Feldmann, R. Rackwitz, E. Heinicke, and H. J. Kaiser, Z. Naturforsch. 32a, 302 (1977).
[7]D. Feldmann, Z. Phys. A 277, 19 (1976).
[8]D. Feldmann, R. Rackwitz, E. Heinicke, and H. J. Kaiser, Z. Phys. A 282, 143 (1977).
[9]H. J. Kaiser, E. Heinicke, R. Rackwitz, and D. Feldmann, Z. Phys. 270, 259 (1974).
[10]D. Feldmann, Z. Naturforsch. 25a, 621 (1970).
[11]M. L. Seman and L. M. Branscomb, Phys. Rev. 125, 1602 (1962).
[12]A. Mandl, Phys. Rev. A 3, 251 (1971).
[13]A. Mandl, Phys. Rev. A 14, 345 (1976).
[14]A. Mandl and H. A. Hyman, Phys. Rev. Lett. 31, 417 (1973).
[15]H.-P. Popp, Z. Naturforsch. 22a, 254 (1967).
[16]G. Mück and H.-P. Popp, Z. Naturforsch. 23a, 1213 (1968).
[17]H. Frank, M. Neiger, and H.-P. Popp, Z. Naturforsch. 25a, 1617 (1970).
[18]B. Steiner, Phys. Rev. 173, 136 (1968).
[19]B. Steiner, M. L. Seman, and L. M. Branscomb, *Atomic Collision Processes* (North-Holland, Amsterdam, 1964), p. 537.
[20]L. M. Branscomb, S. J. Smith, and G. Tisone, J. Chem. Phys. 43, 2906 (1965).
[21]W. C. Lineberger and B. W. Woodward, Phys. Rev. Lett. 25, 424 (1970).
[22]H. Hotop, T. A. Patterson, and W. C. Lineberger, Phys. Rev. A 8, 762 (1973).
[23]A. R. P. Rau and U. Fano, Phys. Rev. A 4, 1751 (1971).
[24]R. M. Stehman and S. B. Woo, Phys. Rev. A 23, 2866 (1981).
[25]J. C. Slater, *Quantum Theory of Atomic Structure* (McGraw-Hill, New York, 1960), Vol. 2, Chap. 21.
[26]That is, the Pauli exclusion principle does not allow some combinations of L and S for electrons having the same radial and orbital angular momentum quantum number, n and l.
[27]Robert M. Stehman, Ph.D. thesis, University of Delaware, 1980 (unpublished).
[28]P. C. Engelking and W. C. Lineberger, Phys. Rev. A 19, 149 (1979).